THE JOURNAL OF PHYSICAL CHEMISTRY B

ARTICLE

pubs.acs.org/JPCB

Peptide-Induced Asymmetric Distribution of Charged Lipids in a Vesicle Bilayer Revealed by Small-Angle Neutron Scattering

Shuo Qian and William T. Heller*

Center for Structural Molecular Biology, Chemical Sciences and Neutron Scattering Science Divisions, Oak Ridge National Laboratory, Oak Ridge, Tennessee 37831, United States

Supporting Information

ABSTRACT: Cellular membranes are complex mixtures of lipids, proteins, and other small molecules that provide functional, dynamic barriers between the cell and its environment, as well as between environments within the cell. The lipid composition of the membrane is highly specific and controlled in terms of both content and lipid localization. The membrane structure results from the complex interplay between the wide varieties of molecules present. Here, small-angle neutron scattering and selective deuterium labeling were used to probe the impact of the membrane-active peptides melittin and alamethicin on the structure of lipid bilayers composed of a mixture of the lipids dimyristoyl phosphatidylglycerol (DMPG) and chain-perdeuterated dimyristoyl phosphatidylcholine (DMPC). We found that both peptides enriched the outer leaflet of the bilayer with the negatively charged DMPG, creating an asymmetric distribution of lipids. The level of enrichment is peptide concentration-dependent and is stronger for melittin than it is for alamethicin. The enrichment between the inner and outer bilayer leaflets occurs at very low peptide concentrations and increases with peptide concentration, including when the peptide adopts a membrane-spanning, pore-forming state. The results suggest that these membrane-active peptides may have a secondary stressful effect on target cells at low concentrations that results from a disruption of the lipid distribution between the inner and outer leaflets of the bilayer that is independent of the formation of transmembrane pores.

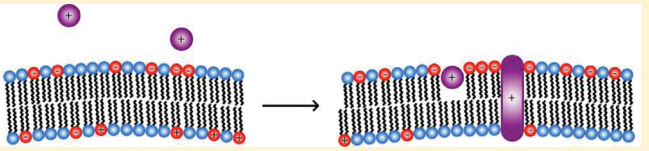

The intricate nature of the cellular membrane continues to challenge researchers hoping to understand the complex interplay between the various constituents that drive structure and function. Cellular membranes consist of lipids, membrane-integral proteins, and other small molecules such as cholesterol in what is referred to as a fluid mosaic structure.[1] The protein−lipid interaction is particularly complex, and simplified systems composed of phospholipids and small, membrane-active peptides are often studied as model systems that can be readily understood.

The lipid composition of the cellular membrane is highly regulated, and a degree of localization is maintained.[1] Native cell membranes have an asymmetric distribution of lipid species between the inner and outer leaflets of the bilayer. The asymmetric distribution does not happen by transmembrane diffusion, which can be very slow for some species of lipids.[2] Instead, membrane proteins exist specifically to transport lipids synthesized inside the cell to the outer leaflet of the bilayer,[3] and small membrane-spanning peptides and proteins can induce such a redistribution even more efficiently.[4,5] The movement of lipids between leaflets of the bilayer, often termed flip-flop, has been observed for melittin,[4] magainin,[6] and other helical peptides.[7,8] Lipid flip-flop has also been observed in simulations of alamethicin.[9] A change in the relative equilibrium populations of lipids caused by poly-L-lysine in surface-adsorbed phosphatidylcholine−phosphatidylserine bilayers was recently observed.[10]

Melittin (mel), a component of honey bee (*A. melifera*) venom, and alamethicin (ala), from *T. viriide*, are two extensively studied membrane-active peptides.[11] Melittin is α-helical and highly charged, making it water soluble. A proline near the middle of the 26 amino acid sequence imparts a helix-turn-helix structure. Alamethicin is also α-helical, but the peptide has a single charged residue, and it is not water soluble. Alamethicin also has a proline that is located $\sim^2/_3$ of the way through the 20 amino acid sequence. Both peptides are known to associate with the polar headgroups of phospholipid bilayers in a lipid-dependent manner[12] and form transmembrane pores in a concentration-dependent manner.[13,14] The peptides alter the structure of the lipid bilayer, such as decreasing the average thickness of the lipid bilayer when the peptides are adsorbed at the surface at low concentrations.[15−17]

Many of these effects have been observed in lipid bilayers composed of a single lipid species and at high peptide concentrations. Here, we report melittin- and alamethicin-induced changes in the structure of bilayers composed of a 7:3 mixture of deuterium-labeled dimyristoyl phosphatidylcholine (d54-DMPC), a zwitterionic lipid, and dimyristoyl phosphatidylglycerol (DMPG), a negatively charged lipid, using small-angle neutron scattering (SANS). The peptide-to-lipid ratios studied here are relatively low compared to those of other studies of their mechanism of action.[18] The SANS data and modeling

Received: May 1, 2011
Revised: July 7, 2011
Published: July 13, 2011

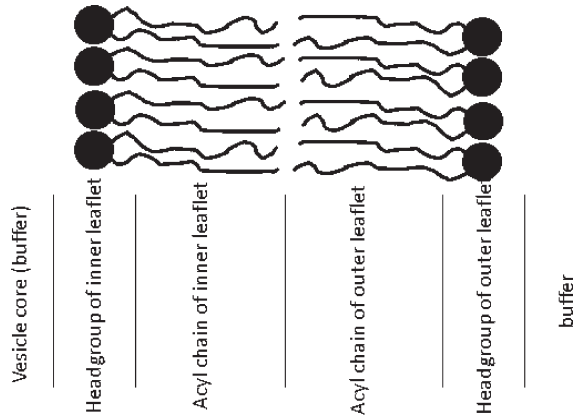

Figure 1. Schematic of the lipid bilayer, defining the regions into which the model is divided.

demonstrate that the presence of both peptides perturbs the distribution of the charged DMPG in the vesicle, with more of the lipid residing in the outer bilayer leaflet in a peptide concentration-dependent manner. The effect is stronger for the highly charged melittin but is still significant for alamethicin. Lipid redistribution takes place at concentrations well below the critical concentration required for pore formation.

MATERIALS AND METHODS

1,2-Dimyristoyl(d54)-*sn*-glycero-3-phosphocholine (d54-DMPC) and 1,2-dimyristoyl-*sn*-glycero-3-phospho-(1′-rac-glycerol) (DMPG) were purchased from Avanti Polar Lipids (Alabaster, AL) in powder form. Alamethicin and melittin were purchased from Sigma-Aldrich (St. Louis, MO). All materials were used without further purification. Samples were prepared for the peptide-free vesicles and for vesicles containing three different peptide-to-lipid ratios (P/L) (1:500, 1:200, and 1:50 for alamethicin and 1:1000, 1:500, and 1:200 for melittin).

Vesicle Preparation. The unilamellar vesicles were prepared by using a miniextruder (Avanti Polar Lipids, Alabaster, AL). The lipid mixtures of d54-DMPC/DMPG = 7:3 (molar ratio) were made and then were dissolved in H_2O/D_2O mixtures at ~1% w/w concentration. To achieve a contrast match of the d54-DMPC, the background solution was a 10% H_2O/90% D_2O (by volume) mixture. Samples were also prepared in 86% H_2O/14% D_2O (by volume), which is the match point of the hydrogenated DMPG. The lipid suspensions underwent at least three freeze−thaw cycles to ensure the extruded vesicles were unilamellar. The peptides were added to the lipid suspensions before the vesicle extrusion. The vesicles were produced by extruding the mixture through a polycarbonate membrane having 100 nm diameter pores at least 10 times. During the extrusion process, the samples were maintained above the gel−liquid phase transition temperature of DMPC (23 °C). The vesicle suspensions were stored at 4 °C for no more than 24 h, if they were not used immediately. The size distribution of the vesicles was determined by dynamic light scattering (DLS) performed using a Wyatt Dawn EOS with a QELS attachment (Wyatt Technology Corp., Santa Barbara, CA) and was found to be 65 ± 5 nm. The size distribution of the vesicles was verified to be unaltered by storage except for samples with relatively high peptide concentration. As a result, alamethicin P/L = 1/50 and melittin P/L = 1/200 samples were used immediately after preparation.

CD Spectroscopy. CD spectroscopy was performed to ensure that the peptides were bound to the lipid vesicles and were properly folded into α-helical structures. The samples used for the SANS measurements that were loaded into 1-mm path length quartz cells were measured at 30 °C with a Jasco J-810 CD spectrometer. The data were collected every 0.5 nm from 185 to 250 nm. Ten scans were averaged to produce the final spectra.

SANS Measurements. SANS experiments were performed at the Bio-SANS of the High Flux Isotope Reactor of the Oak Ridge National Laboratory.[19] SANS data were taken at sample-to-detector distances of 1.1 and 6.8 m. The neutron wavelength, λ, was set to 6 Å, and the wavelength spread, $\Delta\lambda/\lambda$, was set to 0.14. Scattered neutrons were collected with a 1 × 1 m two-dimensional (2D) position-sensitive detector having 192 × 192 pixels (ORDELA, Inc., Oak Ridge, TN). The vesicle suspensions and associated background solutions were measured at 30 °C in 1 mm path-length quartz cells (Hellma U.S.A., Plainview, NY). The 2D data were corrected for detector pixel sensitivity, as well as the dark current, which originates from ambient background radiation and the detector's electronic noise. The scattering of the background solution was subtracted from the sample scattering to produce the reduced data. The 2D reduced data were azimuthally averaged to yield the one-dimensional (1D) scattering intensity $I(q)$ vs q, where $q = 4\pi \sin(\theta/\lambda)$ and 2θ is the scattering angle from the incident beam. The 1D profiles from the two detector distances were merged to produce a complete scattering intensity, using software developed at the National Institute of Standards and Technology.[20] A constant background representing the difference in incoherent scattering resulting from the differences in hydrogen content of the samples and backgrounds was subtracted from the 1D profile.

SANS Data Analysis and Modeling. The thickness of the bilayer was analyzed using the modified Kratky−Porod (MKP) approach,[21] which relates the radius of gyration to the thickness of the bilayer and is independent of other model fitting. In addition, the SANS data were fit using a spherical core−shell model to detect an asymmetric distribution of lipids between the inner and outer leaflets of the bilayer. All of the SANS data can be divided into two regions. The low-q data arises from the structure of the vesicles themselves, while the high-q data derives from the internal structure of the bilayer[22] and can be used to probe changes that take place in response to the peptides. To model the structure, four shells were used that represent the lipid headgroup and hydrophobic chain regions of the inner leaflet and the hydrophobic chain and headgroup regions of the outer leaflet of the bilayer, as shown in Figure 1. The core of the model contains the same solution background as exists outside of the vesicles. Table 1 contains the neutron scattering lengths and volumes of the various components in the system that were used to calculate the scattering length densities (SLDs) in the model.

The scattering intensity from the four shell model is given by eq 1:

$$I(q) = A\left[\sum_{i=1}^{5} \frac{3V_i(\rho_i - \rho_{i-1})j_1(qd_i)}{qd_i}\right]^2 S(q) + bkg \qquad (1)$$

In the equation, A and bkg are a scale factor and constant background, respectively. The ρ_i are the SLDs of each shell, and ρ_0 is the neutron scattering length density of the core, which is equal to that of the background buffer solution. V_i is the volume of each shell and $j_1(x)$ is the Bessel function. The d_i (i = 1, 2, 3, 4,

Table 1. Volumes and Neutron Scattering Lengths of the Various Components in the System Used To Calculate SLDs in the Model[a]

component	vol (A^{-3})	scattering length (fm)
melittin	3445[42]	559.53
alamethicin	2381[42]	401.72
PC headgroup	320[43]	60.09
PG headgroup	300[44]	86.70
d-54 lipid chain	780[43]	533.16
lipid chain	780[43]	−29.06
D_2O	30	19.14
H_2O	30	−1.68

[a] The total scattering lengths and SLDs are calculated from neutron scattering lengths provided by Sears.[41]

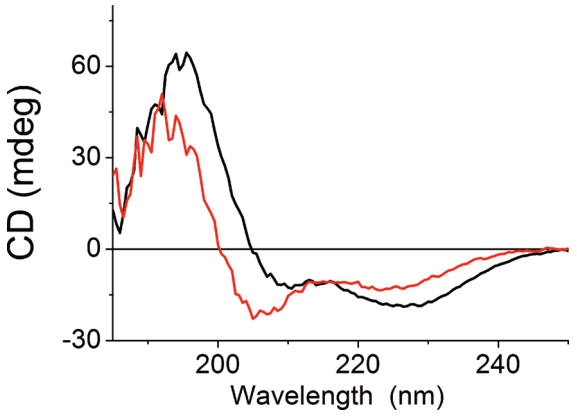

Figure 2. CD spectra of alamethcin (black) and melittin (red) in d54-DMPC/DMPG vesicles.

5) are the radii of the shells in the model, being the inner vesicle radius, the thickness of the headgroup and chain region of inner leaflet, and the thickness of the headgroup and chain region of the outer leaflet, respectively. $S(q)$ is the structure factor between vesicles and is equal to unity ($S(q) = 1$) for the dilute vesicle solutions measured in this experiment.

The SLD of the headgroup of the inner leaflet is given by the following:

$$\rho_{\text{in, head}} = \frac{(b_{\text{pc}}r_{\text{dmpc}} + b_{\text{pg}}r_{\text{dmpg}}) + N_{\text{w}}b_{\text{buffer}} + r_{\text{peptide}}b_{\text{peptide}}(1 - r_{\text{peptide, inserted}})(P/L)}{(V_{\text{pc}}r_{\text{dmpc}} + V_{\text{pg}}r_{\text{dmpg}}) + N_{\text{w}}V_{\text{buffer}} + r_{\text{peptide}}V_{\text{peptide}}(1 - r_{\text{peptide, inserted}})(P/L)} \quad (2)$$

in which r_{dmpc} and r_{dmpg} are the molar fraction of d54-DMPC and DMPG within the inner leaflet; thus, $r_{\text{dmpg}} = 1 - r_{\text{dmpc}}$. The d54-DMPC/DMPG mixture is a 7:3 molar ratio, so if the bilayer is homogeneous between the two leaflets, r_{dmpg} should be 0.3 and r_{dmpc} should be 0.7. A deviation from these values implies asymmetric distribution of the two lipid components between the inner and outer leaflets of the bilayer. b_{pc} and b_{pg} are the scattering length densities of the PC and PG headgroups, respectively. N_{w} is the number of water molecules in the headgroup region of each leaflet; b_{buffer} is the scattering length density of the background buffer solution. r_{peptide} is the ratio of peptide attached to the inner leaflet. The positively charged peptides are expected to preferentially associate with the PG headgroups, so r_{peptide} is proportional to the ratio of PG in the inner leaflet. $r_{\text{peptide,inserted}}$ is the ratio of peptide inserted into the chain region and is a free parameter in the model fitting. P/L is the peptide-to-lipid ratio. The V_i are the corresponding molecular volumes of the respective components. The SLD of the chain region of the inner leaflet is given by the following:

$$\rho_{\text{in, chain}} = \frac{(b_{\text{dmpc, chain}}r_{\text{dmpc}} + b_{\text{dmpg, chain}}r_{\text{dmpg}}) + (r_{\text{peptide}}b_{\text{peptide}}r_{\text{peptide, inserted}})(P/L)}{(V_{\text{dmpc, chain}}r_{\text{dmpc}} + V_{\text{dmpg, chain}}r_{\text{dmpg}}) + (r_{\text{peptide}}V_{\text{peptide}}r_{\text{peptide, inserted}})(P/L)} \quad (3)$$

For the outer leaflet, the SLDs are calculated in a similar way. It is important to note that the model does not account for the effect of transmembrane pores on the scattering length density. A transmembrane pore alters the SLD of all layers by a constant, producing no effect on the bilayer asymmetry. The constant would be particularly small for most of the samples measured with the exception of alamethicin at $P/L = 1/50$, given the relatively low P/L values studied.

The unilamellar vesicles produced by extrusion are not uniform in size; therefore, the polydispersity of the vesicles is accounted for by convoluting the model described above with the nonsymmetrical Schulz distribution shown in eq 4:

$$I(q, \langle R\rangle) = \frac{\int_{r_{\text{min}}}^{r_{\text{max}}} I(q, R)\, G(R, \langle R\rangle)\, \mathrm{d}R}{\int_{r_{\text{min}}}^{r_{\text{max}}} G(R, \langle R\rangle)\, \mathrm{d}R} \quad (4)$$

in which $G(R,\langle R\rangle)$ is the Schultz distribution: $G(R,\langle R\rangle) = R^m/m!\,((m+1)/\langle R\rangle)^{m+1}\mathrm{e}^{((m+1)R)/\langle R\rangle}$, where $m = (1/\sigma^2) - 1$; σ is the relative standard deviation of the vesicle radius, $\sigma = \sigma_R/R$; and R is the radius of the core of the vesicle. Previous studies on scattering from vesicles[21−23] have shown that the scattering is sensitive to the vesicle size for $q < 0.01$ A^{-1}. As a result, the precise vesicle radius and polydispersity have little effect on the fitting parameters related to the bilayer thickness. Therefore, we used the average radius of 65 nm determined from the DLS measurements and employed a typical polydispersity of unilamellar vesicles,[24] $\sigma_R = 30\%$, for the fitting. Because we are only interested in changes in the local bilayer structure induced by the peptides, we focused on fitting the $q > 0.03$ A^{-1} region.

The instrument resolution function is also taken into account by convoluting $I(q,\langle R\rangle)$ with the Gaussian instrument resolution function shown in eq 5:

$$I(q) = \int \frac{1}{\sigma_q(q)\sqrt{2\pi}}\, \mathrm{e}^{-(q' - q)^2/\sigma_q(q)^2} I(q')\, \mathrm{d}q' \quad (5)$$

dx.doi.org/10.1021/jp204045t |J. Phys. Chem. B 2011, 115, 9831–9837

Table 2. Bilayer Thickness Characterization by Modified Kratky–Porod Method (in Å)

	90% D_2O	14% D_2O
lipid only	48.9 ± 1.0	28.0 ± 1.0
ala 1/500	48.4 ± 1.0	27.7 ± 1.0
ala 1/200	48.1 ± 1.0	27.7 ± 1.0
ala 1/50	47.4 ± 1.0	26.9 ± 1.0
mel 1/1000	49.1 ± 1.0	26.8 ± 1.5
mel 1/500	47.6 ± 1.0	27.5 ± 1.5
mel 1/200	49.6 ± 1.0	27.7 ± 1.5

where $\sigma_q(q)$ is the uncertainty in the value of q from the instrument.

Data fitting was accomplished by first using the lsqcurvefit function in MATLab software (MathWorks, Inc., Natick, MA), which performs nonlinear, least-squares curve fitting. During the procedure, the undetermined model parameters, such as the thickness of each of the layers d1, d2, d3, and d4, are given constraints to avoid unphysical results. After performing searches from several initial values, we then manually change the parameters slightly to improve the fitting by comparing the experimental data and the model, which was accomplished through the use of χ^2 that is defined in eq 6:

$$\chi^2 = \frac{1}{N-p}\sum_{i=1}^{N}\left[\frac{I_{\text{model}}(q) - I_{\text{exp}}(q)}{\sigma_{\text{exp}}(q)}\right]^2 \quad (6)$$

where N is the number of data points, p is the number of parameters in the model, and $\sigma_{\text{exp}}(q)$ is the experimental uncertainty in the data. The uncertainties of the structural parameters are estimated from the difference between the manual fitting results and automatic fitting. The model parameters employed in the fitting were the thickness of each layer, d_i, the molar ratio of d54-DMPC in the inner leaflet, r_{dmpc}, the number of waters associated with each lipid headgroup, N_w, as well as the overall scale factor and background (eq 1).

RESULTS

The CD spectra collected for the two peptides bound to the d54-DMPC/DMPG vesicles are shown in Figure 2. Alamethicin adopts a predominantly helical conformation, consistent with previously published data.[25]. In contrast, the CD spectrum of melittin is consistent with a mixture of α-helix and random coil. The peptide is random coil in solution but adopts a conformation similar to the one adopted here when bound to vesicles.[26] The results indicate that the peptides are bound to the vesicles and are not free in solution.

The bilayer thicknesses for the series of samples measured were determined from the SANS data collected in 90% D_2O and 14% D_2O by using the MKP method.[21] The model-independent thicknesses are presented in Table 2, while the MKP plots are shown in Figure S1 in the Supporting Information. Note that the thicknesses determined from 14% D_2O samples are much smaller than those determined from the 90% D_2O data, which is due to the fact that the d54-DMPC is matched out in 90% D_2O, so most of the scattering signal is from the hydrogenated DMPG. Thus, the thickness is more representative of the total bilayer thickness. However, in 14%D_2O, the scattering signal arises from the deuterium-labeled DMPC chains, which results in a thickness

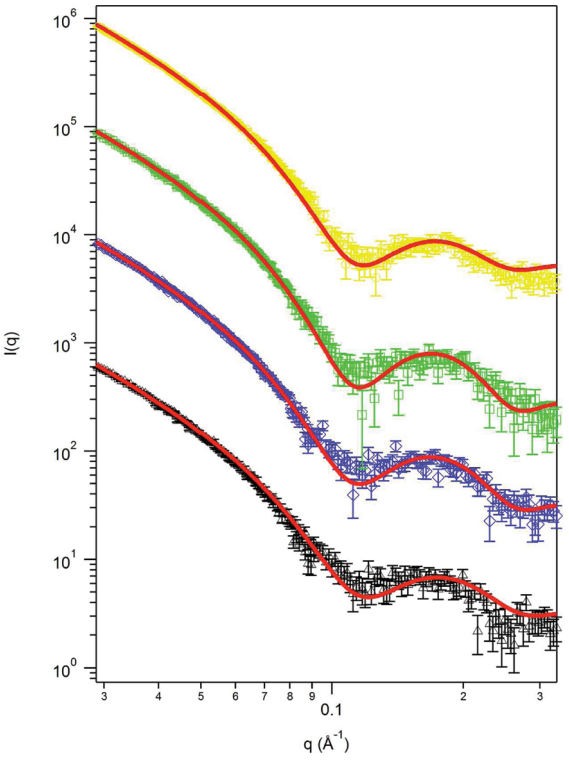

Figure 3. SANS data of alamethicin in d54-DMPC/DMPG vesicles. Curves, offset for clarity: lipid only (yellow); P/L = 1/500 (green); 1/200 (blue); and 1/50 (black). Red lines are the model fits.

less than that of the bilayer. The two sets of results display consistent trends. The results demonstrate that alamethicin thins the membrane, even when the peptide adopts the pore forming state at P/L = 1/50.[13] Melittin does induce concentration-dependent membrane thinning at the lowest concentrations measured. Interestingly, at the highest concentration studied, 1/200, the thickness of the bilayer becomes greater than the peptide-free bilayer, suggesting that the membrane actually thickens to accommodate the transmembrane conformation of melittin.

The SANS data collected for vesicles containing alamethicin and melittin in 90% D_2O are shown in Figures 3 and 4, respectively. The solid curves shown in the figures are the results of fitting the model described in the Materials and Methods section to the SANS data collected in 90% D_2O. The SANS data collected in 14% D_2O were not suitable for this analysis because the strong incoherent neutron scattering that results from the high hydrogen content of the samples washed out the higher-q features in the data (shown in Figures S2 and S3 in the Supporting Information). The structural parameters found by the model fitting are summarized in Table 3. As can be seen in the Results section for the peptide-free lipid vesicles, the d54-DMPC found in the inner leaflet of the bilayer is nearly consistent with the expected molar ratio for a homogeneous distribution of the lipids. The symmetry of the peptide-free bilayer is consistent with previous studies that show a symmetric bilayer and constant thickness in phosphatidylcholine–phosphatidylserine lipid vesicles having a wide range of diameters.[23] In the case of alamethicin, the differences in the region of the SANS data resulting from the internal structure of the bilayer that were caused by the peptide are subtle. The position of the first minima in the best fit

to the data (the solid curve) does not change a great deal at P/L = 1/500 and 1/200, which can also be seen in the fitting parameters presented in Table 3, even though the fitting found that roughly half of the population of alamethicin adopted a transmembrane state. At P/L = 1/50, alamethicin thins the lipid bilayer, which is consistent with the known behavior of alamethicin.[27] Interestingly, the amount of water in the headgroup region of the bilayer decreases with increasing peptide content, which suggests that the presence of the peptide in the membrane displaces water from the headgroup region of the bilayer.

Much like alamethicin, melittin does not produce a large change in the bilayer structure at low concentrations, but changes begin to take place at a lower concentration than that for alamethicin. Melittin is sufficiently disruptive that samples produced at P/L = 1/50 were not suitable enough to provide acceptable SANS data for this analysis. Again, the peptide is displacing water in the headgroup region of the bilayer, although the amount of water displaced by melittin is larger than that for alamethicin at P/L = 1/200. Surprisingly, the d54-DMPC/DMPG bilayer thickens by over 4 Å once melittin adopts a membrane-spanning state. The results indicate that the adoption of the transmembrane state has forced the hydrophobic region of the bilayer to stretch in order to accommodate the transmembrane melittin. This is an unexpected result in light of the fact that melittin has a proline hinge near the middle of its sequence that could allow the peptide to bend in order to accommodate the lipid bilayer thickness.[28]

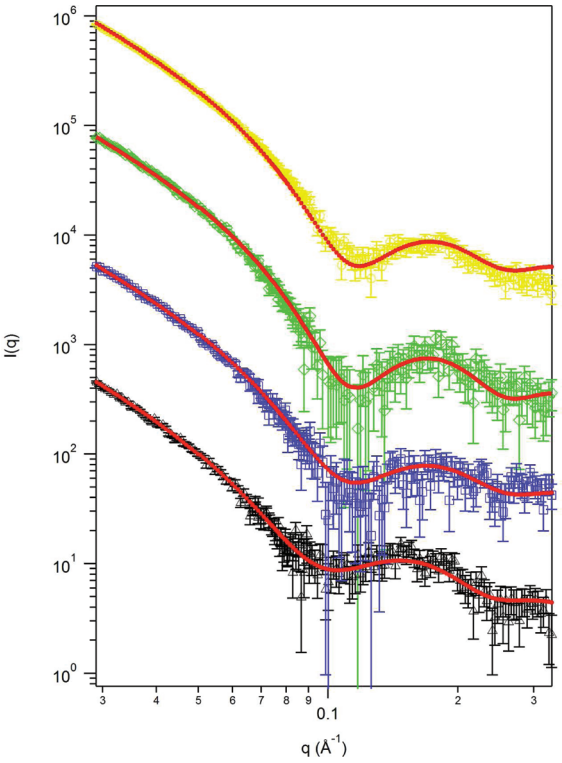

Figure 4. SANS data of melittin in d54-DMPC/DMPG vesicles. Curves, offset for clarity: lipid only (yellow); P/L = 1/1000 (green); 1/500 (blue); and 1/200 (black). Red lines are the model fits.

Both peptides induce an asymmetric distribution of charged lipid in the membrane. Alamethicin creates considerable lipid asymmetry even at low concentrations, and the asymmetry continues to increase once alamethicin adopts a transmembrane state. The highly charged melittin produces a larger redistribution of the charged lipid at P/L = 1/200 than alamethicin, where both peptides are estimated to exist in a 50% surface adsorbed/50% transmembrane state. The strong asymmetry observed for melittin suggests that not all of the lipid movement is driven by binding to surface-absorbed peptides. This conclusion is supported by the asymmetry seen for alamethicin when 90% of the peptide in the bilayer has adopted a pore-forming, transmembrane state.

DISCUSSION

The results presented here demonstrate that the equilibrium distribution of charged lipids in a phospholipid vesicle bilayer is altered by the membrane-active peptides alamethicin and melittin, resulting in an enrichment of charged lipids in the outer leaflet of the vesicle. The enrichment from the equilibrium distribution that results during the formation of the vesicles, which shows a very slight asymmetry without any peptides that could be the result of curvature strain,[29,30] begins at peptide concentrations well below the critical concentration for the formation of the transmembrane pores. Rather than returning to a uniform distribution once this critical concentration for pore formation is reached, the enrichment continues to increase. The membrane-active peptides are better able to recruit charged lipids from one leaflet of the bilayer to the other once pore formation takes place.[31] Melittin produces a stronger effect than alamethicin, consistent with it being the more disruptive and charged of the two peptides.

In the absence of membrane-active peptides, the rate of lipid flip-flop is slow and depends on the composition of the bilayer.[32] Membrane-active peptides, including alamethicin and melittin,

Table 3. Structural Parameters Obtained by Fitting the SANS Data Using the Model[a]

P/L		lipid only	ala 1/500	ala 1/200	ala 1/50	mel 1/1000	mel 1/500	mel 1/200
inner leaflet	headgroup (Å)	8.10	8.10	8.0	7.84	8.10	8.10	8.20
	chain (Å)	14.20	14.10	14.08	13.60	14.20	14.10	15.90
outer leaflet	chain (Å)	14.20	14.10	14.10	13.50	14.20	13.90	16.00
	headgroup (Å)	8.10	8.15	8.00	7.86	8.10	8.10	8.30
total shell thickness (Å)		44.60	44.45	44.18	42.80	44.60	44.20	48.40
N_w		6.50 ± 0.50	3.95 ± 0.05	3.15 ± 0.05	3.15 ± 0.14	5.00 ± 0.50	4.00 ± 0.50	2.00 ± 0.50
peptide insertion ratio (%)		0	0	50 ± 10	90 ± 10	0	35 ± 15	60 ± 15
DMPC ratio of inner leaflet (%)		76 ± 2	78 ± 2	79 ± 2	85 ± 2	75 ± 2	79 ± 2	89 ± 2

[a] The shell thickness is the sum of the headgroup and chain thickness of both inner and outer leaflets. The uncertainty in the various thicknesses is estimated to be ±0.2 Å, and the various shells are highly correlated. The uncertainty in the total shell thickness is estimated to be less than 1 Å. N_w is the number of waters associated per lipid headgroup.

dx.doi.org/10.1021/jp204045t |J. Phys. Chem. B 2011, 115, 9831–9837

greatly increase the rate of flip-flop,[33−35] and the translocation of phospholipids induced by helical peptides has been studied.[36−38] Here the results demonstrate that the membrane-active peptides not only change the distribution of lipids in a mixed lipid membrane but also maintain the asymmetric distribution in the equilibrium state of the vesicle. At low peptide concentrations, the peptides are likely to be driven to the surface to release curvature strain in the vesicles. Movement of the charged lipids can then be thought of in terms of charge neutralization. The increased redistribution driven by melittin is consistent with its much higher net charge. A recent simulation of mixed lipid bilayers shows charged lipid domain formation in mixed bilayers in response to the cationic, helical, membrane-active peptide Ltc1.[39] In lipid mixtures containing dioleoyl phosphatidylethanolamine (DOPE), a zwitterionic lipid, and dioleoyl phosphatidylglycerol (DOPG) at a 7:3 molar ratio, the peptide increases the average size of DOPG clusters in the membrane, consistent with the lipid redistributions seen at low concentrations. The additional enrichment of charged lipids in the outer leaflet of the bilayer that takes place at concentrations consistent with transmembrane pore formation is somewhat surprising considering the expected increase in the rate of lipid flip-flop. An increased rate of flip-flop would allow the charged lipids to migrate to a configuration that minimizes the charge repulsion between the lipids, which would be possible if more lipids are on the outer surface of the vesicle. Further, any peptides not in a transmembrane state, being directly involved in the structure of the pores, will prefer to be on the surface of the vesicle to relieve curvature strain, which drives the charged lipids there to provide some charge neutralization.

While the predominant mechanism of action of alamethicin and melittin seems to be the perturbation of the membrane and the formation of transmembrane pores,[13] the present results show that the distribution of charged lipids in the inner and outer leaflets of the bilayer can be modified by a membrane-active peptide, particularly once transmembrane pores are formed. The redistribution of lipids in the membrane is an additional stressor on the cell beyond the impact of the peptide-formed pores on the transmembrane potential maintained by cells. The fact that the simple presence of a peptide at very low concentrations in a surface-adsorbed state produces the effect has interesting implications. For instance, the disruption of the natural lipid distribution has been shown to be an important step during apoptosis.[40] The current results suggest that small cationic membrane-bound peptides can affect cellular signaling simply by binding to the surface of a cell.

■ ASSOCIATED CONTENT

Supporting Information. Modified Kratky−Porod fits to determine the bilayer thickness and SANS data from vesicle−peptide samples prepared in 14% D_2O. This material is available free of charge via the Internet at http://pubs.acs.org.

■ AUTHOR INFORMATION

Corresponding Author

*Phone: 865-241-0093. Fax: 865-574-8363. E-mail: hellerwt@ornl.gov.

■ ACKNOWLEDGMENT

The authors would like to thank H. M. O'Neill for use of the CD instrument. This research at Oak Ridge National Laboratory's Center for Structural Molecular Biology (Project ERKP291) was supported by the Office of Biological and Environmental Research using facilities supported by the U.S. Department of Energy, managed by UT-Battelle, LLC under Contract No. DE-AC05-00OR22725.

■ REFERENCES

(1) Engelman, D. M. *Nature* **2005**, *438*, 578–580.
(2) Devaux, P. F. *Biochemistry* **1991**, *30*, 1163–1173.
(3) Nagao, K.; Kimura, Y.; Mastuo, M.; Ueda, K. *FEBS Lett.* **2010**, *584*, 2717–2723.
(4) Fattal, E.; Nir, S.; Parente, R. A.; Szoka, F. C. *Biochemistry* **1994**, *33*, 6721–6731.
(5) Anglin, T. C.; Brown, K. L.; Conboy, J. C. *J. Struct. Biol.* **2009**, *168*, 37–52.
(6) Matsuzaki, K.; Murase, O.; Fujii, N.; Miyajima, K. *Biochemistry* **1996**, *35*, 11361–11368.
(7) Kol, M. A.; de Kroon, A.; Rijkers, D. T. S.; Killian, J. A.; de Kruijff, B. *Biochemistry* **2001**, *40*, 10500–10506.
(8) Kol, M. A.; de Kroon, A.; Killian, J. A.; de Kruijff, B. *Biochemistry* **2004**, *43*, 2673–2681.
(9) Sapay, N.; Bennett, W. F. D.; Tieleman, D. P. *Biochemistry* **2010**, *49*, 7665–7673.
(10) Brown, K. L.; Conboy, J. C. *J. Am. Chem. Soc.* **2011**, *133*, 8794–8797.
(11) Bechinger, B. *J. Membr. Biol.* **1997**, *156*, 197–211.
(12) Shai, Y. *Biochim. Biophys. Acta, Biomembr.* **1999**, *1462*, 55–70.
(13) Huang, H. W. *Biochemistry* **2000**, *39*, 8347–8352.
(14) Qian, S.; Wang, W.; Yang, L.; Huang, H. W. *Biophys. J.* **2008**, *94*, 3512–3522.
(15) Dawson, C. R.; Drake, A. F.; Helliwell, J.; Hider, R. C. *Biochim. Biophys. Acta* **1978**, *510*, 75–86.
(16) Wu, Y. L.; He, K.; Ludtke, S. J.; Huang, H. W. *Biophys. J.* **1995**, *68*, 2361–2369.
(17) He, K.; Ludtke, S. J.; Heller, W. T.; Huang, H. W. *Biophys. J.* **1996**, *71*, 2669–2679.
(18) Lee, M. T.; Chen, F. Y.; Huang, H. W. *Biochemistry* **2004**, *43*, 3590–3599.
(19) Lynn, G. W.; Heller, W.; Urban, V.; Wignall, G. D.; Weiss, K.; Myles, D. A. A. *Phys. B* **2006**, *385−86*, 880–882.
(20) Kline, S. R. *J. Appl. Crystallogr.* **2006**, *39*, 895–900.
(21) Balgavy, P.; Dubnickova, M.; Kucerka, N.; Kiselev, M. A.; Yaradaikin, S. P.; Uhrikova, D. *Biochim. Biophys. Acta, Biomembr.* **2001**, *1512*, 40–52.
(22) Kiselev, M. A.; Zemlyanaya, E. V.; Aswal, V. K.; Neubert, R. H. H. *Eur. Biophys. J.* **2006**, *35*, 477–493.
(23) Kucerka, N.; Pencer, J.; Sachs, J. N.; Nagle, J. F.; Katsaras, J. *Langmuir* **2007**, *23*, 1292–1299.
(24) Kucerka, N.; Nagle, J. F.; Feller, S. E.; Balgavy, P. *Phys. Rev. E: Stat., Nonlinear, Soft Matter Phys.* **2004**, *69*, 051903.
(25) Vogel, H. *Biochemistry* **1987**, *26*, 4562–4572.
(26) Ladokhin, A. S.; Fernández-Vidal, M.; White, S. H. *J. Membr. Biol.* **2010**, *236*, 247–253.
(27) Huang, H. W.; Chen, F. Y.; Lee, M. T. *Phys. Rev. Lett.* **2004**, *92*, 198304.
(28) Weiss, T. M.; van der Wel, P. C.; Killian, J. A.; Koeppe, R. E., 2nd; Huang, H. W. *Biophys. J.* **2003**, *84*, 379–385.
(29) Thomas, P. D.; Poznansky, M. J. *Biochim. Biophys. Acta, Biomembr.* **1989**, *978*, 85–90.
(30) Perlmutter, J. D.; Sachs, J. N. *J. Am. Chem. Soc.* **2011**, *133*, 6563.
(31) Huang, H. W. *Biochim. Biophys. Acta* **2006**, *1758*, 1292–1302.
(32) McConnell, H. M.; Kornberg, R. D. *Biochemistry* **1971**, *10*, 1111–1120.
(33) Fattal, E.; Nir, S.; Parente, R. A.; Szoka, F. C., Jr. *Biochemistry* **1994**, *33*, 6721–6731.
(34) Anglin, T. C.; Brown, K. L.; Conboy, J. C. *J. Struct. Biol.* **2009**, *168*, 37–52.
(35) Sapay, N.; Bennett, W. F.; Tieleman, D. P. *Biochemistry* **2010**, *49*, 7665–7673.

(36) Kol, M. A.; van Laak, A. N. C.; Rijkers, D. T. S.; Killian, J. A.; de Kroon, A. I. P. M.; de Kruijff, B. *Biochemistry* **2003**, *42*, 231–237.
(37) Kol, M. A.; de Kroon, A. I.; Killian, J. A.; de Kruijff, B. *Biochemistry* **2004**, *43*, 2673–2681.
(38) Kol, M. A.; de Kroon, A. I.; Rijkers, D. T.; Killian, J. A.; de Kruijff, B. *Biochemistry* **2001**, *40*, 10500–10506.
(39) Polyansky, A. A.; Ramaswamy, R.; Volynsky, P. E.; Sbalzarini, I. F.; Marrink, S. J.; Efremov, R. G. *J. Phys. Chem. Lett.* **2010**, *1*, 3108–3111.
(40) Fadok, V. A.; de Cathelineau, A.; Daleke, D. L.; Henson, P. M.; Bratton, D. L. *J. Biol. Chem.* **2001**, *276*, 1071–1077.
(41) Sears, V. *Neutron News* **1992**, *3*, 29–37.
(42) Chazan, A. *Peptide Property Calculator*; Northwestern University: Evanston, IL, http://www.basic.northwestern.edu/biotools/proteincalc.html.
(43) Armen, R. S.; Uitto, O. D.; Feller, S. E. *Biophys. J.* **1998**, *75*, 734–744.
(44) Marra, J. *Biophys. J.* **1986**, *50*, 815–825.